STAR Protocols

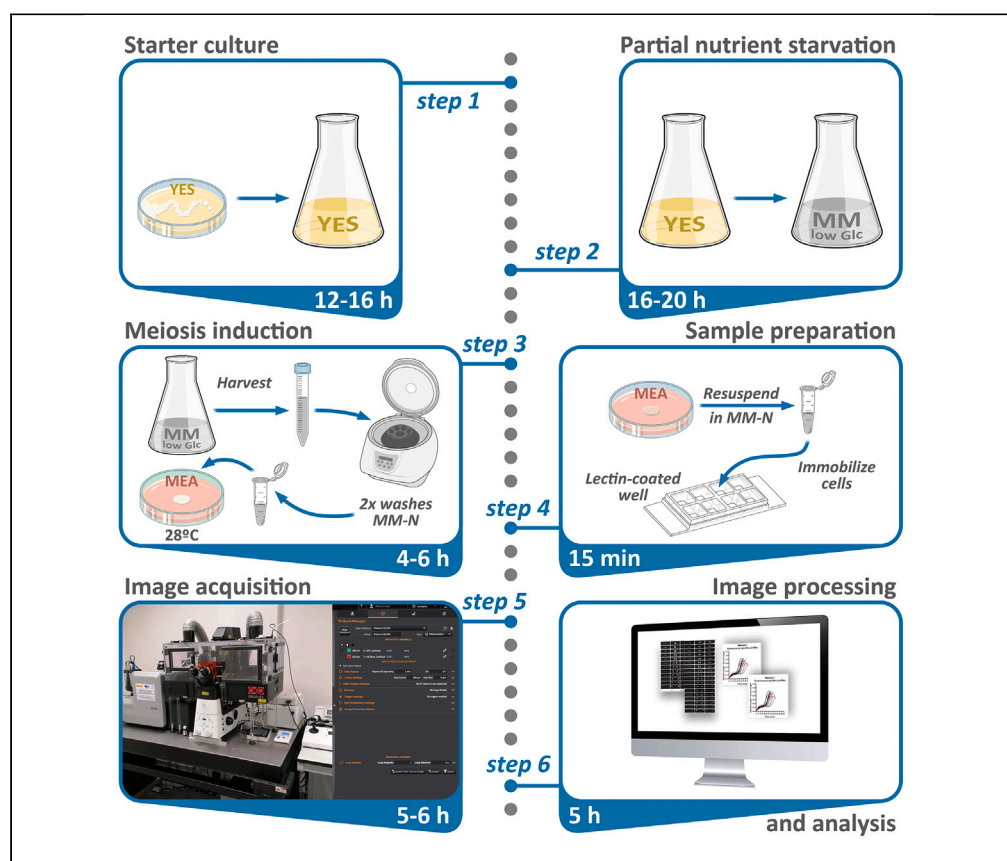**Protocol**

Analyzing self-assembled spindle dynamics in fission yeast meiosis using *in vivo* fluorescence imaging

Alberto Pineda-Santaella, Rebeca Martín-García, Alfonso Fernández-Álvarez

alfonso.fernandez.alvarez@csic.es

Highlights

Workflow for live microscopy of self-assembled spindles in fission yeast meiosis

Maximize meiocyte numbers showing self-assembled spindles

Guidelines for measuring self-assembled spindle occurrences

Chromosome segregation in female meiosis in many metazoans is mediated by acentrosomal spindles. The analysis of the dynamics of self-assembled spindles is a challenge due to the low availability of oocytes. Here, we present a protocol for analyzing self-assembled spindle dynamics in fission yeast meiosis using *in vivo* fluorescence imaging. We describe steps for starter culture preparation, meiosis induction, and sample preparation. We then detail procedures for acquisition and analysis of images of self-assembled spindles.

Publisher's note: Undertaking any experimental protocol requires adherence to local institutional guidelines for laboratory safety and ethics.

Protocol

Analyzing self-assembled spindle dynamics in fission yeast meiosis using *in vivo* fluorescence imaging

Alberto Pineda-Santaella,[1] Rebeca Martín-García,[1,2] and Alfonso Fernández-Álvarez[1,3,*]

[1]Instituto de Biología Funcional y Genómica (IBFG), Consejo Superior de Investigaciones Científicas (CSIC) and Universidad de Salamanca, Calle Zacarías González 2, 37007 Salamanca, Spain

[2]Technical contact: rebemg@usal.es

[3]Lead contact

*Correspondence: alfonso.fernandez.alvarez@csic.es
https://doi.org/10.1016/j.xpro.2023.102655

SUMMARY

Chromosome segregation in female meiosis in many metazoans is mediated by acentrosomal spindles. The analysis of the dynamics of self-assembled spindles is a challenge due to the low availability of oocytes. Here, we present a protocol for analyzing self-assembled spindle dynamics in fission yeast meiosis using *in vivo* fluorescence imaging. We describe steps for starter culture preparation, meiosis induction, and sample preparation. We then detail procedures for acquisition and analysis of images of self-assembled spindles.

For complete details on the use and execution of this protocol, please refer to Pineda-Santaella and Fernández-Álvarez (2019)[1] and Pineda-Santaella et al. (2021).[2]

BEFORE YOU BEGIN

This protocol outlines the specific steps for inducing meiosis in homothallic (h^{90}, self-sporulating) haploid cells of fission yeast (*Schizosaccharomyces pombe*). However, it is also applicable to heterothallic (h^{-} or h^{+}, non-self-sporulating) cells by mixing cells of both mating types.[3]

To investigate the formation of self-assembled meiotic spindles, it is necessary to create a condition where the spindle pole bodies (SPBs) are unable to nucleate bipolar spindle formation specifically during meiosis. In fission yeast, the formation of bipolar spindles in both mitosis and meiosis relies on localized disassembly of the nuclear envelope beneath the SPBs (similar to the nuclear envelope breakdown stage in metazoans), enabling microtubule-chromosome interactions.[4–6] This disassembly is triggered by the interaction between centromeres (in mitosis) and telomeres (in meiosis) with the SUN-domain protein, Sad1, located at the SPB.[7] To disrupt the interaction between telomeres and Sad1, we use the *sad1* allele Sad1.2, in combination with the loss of *bqt1*, a meiosis-prophase-specific protein involved in maintaining the association between telomeres and Sad1.[8] Consequently, meiocytes with the *bqt1Δ sad1.2* genotype lose the interaction between the SPB and telomeres, leading to compromised localized disassembly of the nuclear envelope.[7,9] Under these conditions, *bqt1Δ sad1.2* meiocytes can assemble a self-organized spindle composed of microtubules (see Figure 1).[1] Remarkably, this spindle is able to segregate chromosomes and operates independently of the SPBs.[1,2]

KEY RESOURCES TABLE

REAGENT or RESOURCE	SOURCE	IDENTIFIER
Chemicals, peptides, and recombinant proteins		
Adenine sulfate	Formedium	DOC0230
Agar	Condalab	1800

(Continued on next page)

Continued

| REAGENT or RESOURCE	SOURCE	IDENTIFIER
Ammonium chloride	Sigma-Aldrich	A9434-500G
Bacto-malt extract	Thermo Fisher	218630
Glucose	PanReac AppliChem	131341.1210
Histidine	Formedium	DOC0145
Lectin from *Glycine max* (soybean)	Sigma-Aldrich	L1395-5MG
Leucine	Formedium	DOC0157
Lysine	Formedium	DOC0171
Potassium hydrogen phthalate	Sigma-Aldrich	179922-500G
Di-sodium phosphate	Sigma-Aldrich	S9763-500G
Uracil	Formedium	DOC0214
Yeast extract	BD Biosciences	212750
Experimental models: Organisms/strains		
S. pombe: SV40-GFP-atb2:leu1 hht1-RFP: kanMX6 his3-D1 ura4-D18 ade6-M216 h⁻	Férnández-Álvarez lab	AFA 3172
S. pombe: SV40-GFP-atb2:leu1 hht1-RFP: kanMX6 his3-D1 ura4-D18 ade6-M216 h⁺	Férnández-Álvarez lab	AFA 3174
S. pombe: SV40-GFP-atb2:leu1 hht1-RFP:kanMX6 sad1-T3S, S52P-13Myc:hphMX6 bqt1::hygMX6 ura4-D18 ade6-M216 h90	Férnández-Álvarez lab	AFA 3170
Software and algorithms		
Adobe Illustrator 2021	Adobe Inc.	https://www.adobe.com/es/products/illustrator.html
Adobe Photoshop 2020	Adobe Inc.	https://www.adobe.com/es/products/photoshop.html
Fiji (v 2.9.0/1.53t)	National Institutes of Health	https://imagej.net/software/fiji/downloads
Fusion software (v 2.4.0.14)	Oxford Instruments-Andor	https://andor.oxinst.com/downloads/view/fusion-release-2.4
Graphpad Prism 8	Dotmatics	https://www.graphpad.com/dl/1057948/D599DCF7/
MetaMorph software	Molecular Devices	https://es.moleculardevices.com/products/cellular-imaging-systems/acquisition-and-analysis-software/metamorph-microscopy
Microsoft Excel 2021	Microsoft	https://support.microsoft.com/es-es/excel
SoftWoRx software (v 7.2.1)	Cytiva	https://download.cytivalifesciences.com/cellanalysis/download_data/softWoRx/7.2.1/SoftWoRx.htm
Other		
35-mm-high μ-dish	ibidi	81156
8-well μ-slide	ibidi	80821
Type F immersion liquid	Leica	11513859
Spinning disk confocal system-Olympus IX81 inverted microscope	Olympus/Yokogawa	N/A
EMMCCD camera	Photometrics	Evolve
Dragonfly 200 confocal microscopy system-Nikon Ti2 E inverted microscope	Nikon/Oxford Instruments-Andor	Dragonfly 200
S-CMOS camera	Oxford Instruments-Andor	Sona
Personal DeltaVision-Olympus IX71inverted microscope	Applied Precision	Personal DeltaVision
Solid State Illumination System	Applied Precision	Insight SSI
CCD camera	Photometrics	CoolSnap HQ2
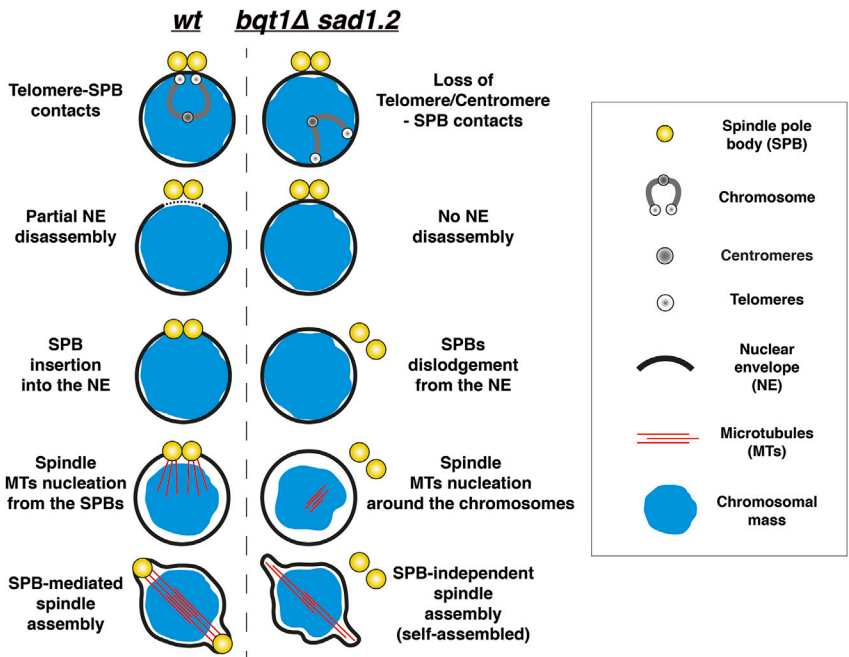
Figure 1. The difference between SPB-dependent (*wt*) and self-assembled spindles (*bqt1Δ sad1.2*) in fission yeast meiosis

Left: the normal (*wt*) process involves SPB insertion into the nuclear membrane and the formation of an SPB-dependent spindle at the beginning of fission yeast meiosis. Right: in the *bqt1Δ sad1.2* mutant, the SPB insertion into the nuclear envelope (NE) and SPB-dependent spindle formation are abolished, resulting in the formation of a self-assembled spindle in meiosis.

MATERIALS AND EQUIPMENT

YES medium (liquid)

Reagent	Final concentration	Amount
Yeast extract	5 g/L	2 g
Histidine	0.225 g/L	0.09 g
Leucine	0.225 g/L	0.09 g
Adenine	0.225 g/L	0.09 g
Uracil	0.225 g/L	0.09 g
Lysine	0.225 g/L	0.09 g
Distilled water (Mili Rho)	N/A	Up to 370 mL

Adjust pH to 5.6 with HCl. Sterilize by autoclaving.

Glucose (400 g/L)	30 g/L	30 mL
Total	N/A	400 mL

Store at no more than 30°C. Maximum time for storage: 6 months.

MEA Medium (solid)

Reagent	Final concentration	Amount
Bacto-malt extract	30 g/L	12 g
Histidine	0.225 g/L	0.09 g
Leucine	0.225 g/L	0.09 g

(Continued on next page)

Continued

Reagent	Final concentration	Amount
Adenine	0.225 g/L	0.09 g
Uracil	0.225 g/L	0.09 g
Distilled water (Mili Rho)	N/A	Up to 400 mL

Adjust pH to 5.5 with NaOH 5 M.

Agar	20 g/L	8 g
Total	N/A	400 mL

Sterilize by autoclaving. Store at no more than 30°C. Maximum time for storage: 6 months.

Minimal Medium without Nitrogen (liquid) (MM-N)

Reagent	Final concentration	Amount
KH Phthalate	3 g/L	1.2 g
Na$_2$HPO$_4$	2.2 g/L	0.88 g
Salts stock (50×)	1×	8 mL
Minerals stock (10000×)	1×	0.04 mL
Distilled water (Mili Rho)	N/A	Up to 380 mL

Adjust pH to 5.6. Sterilize by autoclaving.
Wait for medium to be ∼ 50°C.

Vitamins stock 1000×	1×	0.4 mL
Glucose (400 g/L)	20 g/L	20 mL
Total	N/A	400 mL

Store at no more than 30°C. Maximum time for storage: 6 months.

Minimal Medium with 1% Glucose and Supplements (liquid)

Reagent	Final concentration	Amount
KH Phthalate	3 g/L	1.2 g
Na$_2$HPO$_4$	2.2 g/L	0.88 g
NH$_4$Cl	5 g/L	2 g
Salts stock (50×)	1×	8 mL
Minerals stock (10000×)	1×	0.04 mL
Distilled water (Mili Rho)	N/A	Up to 390 mL

Adjust pH to 5.6. Sterilize by autoclaving.
Wait for medium to be ∼ 50°C.

Vitamins stock 1000×	1×	0.4 mL
Glucose (400 g/L)	10 g/L	10 mL
Histidine	0.225 g/L	0.09 g
Leucine	0.225 g/L	0.09 g
Adenine	0.225 g/L	0.09 g
Uracil	0.225 g/L	0.09 g
Lysine	0.225 g/L	0.09 g
Total	N/A	400 mL

Store at no more than 30°C. Maximum time for storage: 6 months.

Salts stock (50×)

Reagent	Final concentration	Amount
$MgCl_2 \cdot 6 H_2O$	53.5 g/L	53.5 g
$CaCl_2 \cdot 2 H_2O$	0.74 g/L	0.74 g
KCl	50 g/L	50 g
$Na_2SO_4 \cdot 10 H_2O$	3.57 g/L	3.57 g
Distilled water (Mili Rho)	N/A	Up to 1 L
Total	N/A	1 L

Store at no more than 30°C. Maximum time for storage: 6 months.

Vitamins stock (1000×)

Reagent	Final concentration	Amount
Ca Pantonetate	1 g/L	1 g
Nicotinic acid	10 g/L	10 g
Inositol	10 g/L	10 g
Biotina	10 mg/L	10 mg
Distilled water (Mili Rho)	N/A	Up to 1 L
Total	N/A	1 L

Store at 4°C. Maximum time for storage: 6 months.

Minerals stock (10000×)

Reagent	Final concentration	Amount
H_3BO_3	5 g/L	2 g
$MnSO_4$	4 g/L	1.6 g
$ZnSO_4 \cdot 7 H_2O$	4 g/L	1.6 g
$FeCl_3 \cdot 6 H_2O$	2 g/L	0.8 g
$H_2MoO_4 \cdot H_2O$	0.4 g/L	0.16 g
KI	1 g/L	0.4 g
$CuSO_4 \cdot 5 H_2O$	0.4 g/L	0.16 g
Citric acid	10 g/L	4 g
Distilled water (Mili Rho)	N/A	Up to 400 mL
Total	N/A	400 mL

Store at no more than 30°C. Maximum time for storage: 6 months.

STEP-BY-STEP METHOD DETAILS

The following protocol is designed to work ideally with a self-sporulating haploid h^{90} strain or with a cross between sexually compatible strains of h^- and h^+ haploid cells.

Revive cells

⏱ Timing: 1–2 days

This step involves monitoring the transition of cells from a physiologically dormant state in a glycerol stock to a state of active metabolism and growth on a solid, nutrient-rich medium plate.

1. Take a small amount of frozen biomass from the glycerol stock of cells (approximately the size of a grain of rice) and place it onto a plate of solid rich medium, such as supplemented yeast extract (YES) medium (e.g., YE5S).[10,11]
2. Leave the biomass to thaw and dry completely.

3. Incubate the plate at a temperature of 25ºC to 32ºC, depending on the requirements of the genetic background (e.g., thermosensitivity), for 1–2 days until a patch of biomass grows.

Starter culture

⏱ Timing: 12–16 h

Cells are transferred from a suboptimal physiological condition for survival and proliferation on a solid, nutrient-rich medium plate to an optimal state of growth in a liquid, nutrient-rich medium.

4. Take a small amount of the grown biomass (approximately the size of a grain of rice) and inoculate it into 5–10 mL of liquid YES medium in a 25–50 mL Erlenmeyer flask.
5. Incubate the culture at a temperature of 25ºC to 30ºC at 200 rpm, depending on the requirements of the genotype (e.g., thermosensitivity), until it reaches saturation, which is typically indicated by an optical density of 1.

Partial nutrient starvation

⏱ Timing: 16–20 h

In order to achieve a more synchronized induction of meiosis, cells are subjected to partial glucose starvation by reducing its concentration from 3% to 1%.

6. Dilute the pre-culture in a new flask in a total volume of 10 mL of fresh MM with 1% glucose and growth the culture for approximately 16–20 h until it reaches an optical density of 0.6–0.8.

⚠ CRITICAL: Allow the cultures to grow for a minimum of two additional generations.

⚠ CRITICAL: Do not dilute this pre-culture (in MM 1% Glucose) to initial O.D lower than 0.01 since poor fission yeast inocule could result in problems to resume growth.

Meiosis induction

⏱ Timing: 4–6 h

The initiation of the meiotic program in cells is triggered when nitrogen is entirely absent from the medium.

Note: We have chosen MEA medium over other sporulating media (such as SPM or SPA), since we have obtained a more robust synchronisation, i.e., a higher percentage of meiocytes after 4–6 h of incubation. As the exchange of mating factors between cells of opposite sexual types is more effective in a solid medium, the most synchronous induction of cell conjugation is attained by growing the cells in liquid culture under partial glucose deprivation and then plating them out onto solid medium.

7. Transfer the culture from its current vessel to a 15 mL tube.
8. Centrifuge the culture at 1000 × *g* for 3 min.
9. Carefully discard the supernatant from the centrifuged culture and then wash the pellet by pipetting an equal volume of minimal medium without nitrogen, MM-N (2% glucose) onto the pellet.

Note: We use MM-N for the washes and for the filmation since it is crucial to maintain the cells in nutrient-poor conditions (specially deprivation of N) to ensure the progression of the

meiotic program throughout prophase and meiotic divisions, otherwise, if a nutrient-rich medium is used, meiocytes could abort such meiotic program and return to vegetative growth.

10. Centrifuge the culture once again at 1000 × g for 3 min.
11. Discard the supernatant from the centrifuged culture and use a pipette to remove any remaining liquid.
12. Resuspend the pellet in 100–150 μL of liquid MM-N, adjusting the volume according to the size of the pellet.
13. Place a 10 μL drop of the resuspended pellet onto a plate of MEA medium and allow the drop to dry.
14. Incubate the plate at a temperature of 28°C for 4–6 h.

Note: Zygotes typically start to appear after approximately 4 h of incubation at 28°C, but this timeframe may vary depending on the strain, incubation temperature, and medium used for conjugation. Temperatures between 25°C and 30°C can be used. Other solid media, such as Sporulation Agar (SPA) medium, can be used for meiosis induction, but in our experience, MEA enables better synchronous and efficient meiocyte formation than SPA.

Sample preparation for microscopy

⏱ **Timing: 15 min**

Following meiosis induction, meiocytes are moved and immobilized within a microscopy chamber for time-lapse fluorescence microscopy.

Note: The selection of the microscopy chamber format depends on whether a small or large volume of medium is needed, which in turn may be affected by factors such as the inclusion of drugs in the sample. To accommodate both scenarios, we include instructions for both the iBidi 8-well μ-slide (for low volume) and the iBidi 35mm high μ-Dish (for high volume) here.

15. Add 10 μL (iBidi 8-well)-50 μL (iBidi 35 mm high μ-Dish) of soy lectin (1 mg/mL) to the center of the chamber bottom and allow it to settle for 2 min.
16. Use a pipette to extract as much of the lectin as possible from the chamber, then allow the remaining residue to air dry.
17. Using a 1 mL pipette tip, gently resuspend a small amount of biomass from the MEA plate (approximately the size of half a grain of rice) in 300 μL of MM-N.
18. Immobilize the cells by placing 100 μL of the prepared suspension onto the lectin-coated microscopy chamber and allow it to settle for 4 min.
19. Wash away the non-immobilized cells (i.e., cells that are suspended and not adhered to the bottom of the chamber by lectin):
    a. For the iBidi 8-well μ-slide:
       i. Add 300 μL of fresh MM-N from one side of the well towards the cell spot at the bottom of the well, in order to wash away the loosely adhered cells, while the strongly adhered cells will remain immobilized.
       ii. Discard the 300 μL of washing medium.
    b. For the iBidi 35 mm high μ-Dish:
       i. Add 1 mL of fresh MM-N from one side of the dish towards the cell spot at the bottom of the dish, to wash away the non-immobilized cells.
       ii. Repeat this step 3 times, discarding the washing medium.
20. Add either 300 μL of MM-N for the iBidi 8-well μ-slide, or 1 mL for the iBidi 35 mm high μ-Dish.

Note: To maintain nitrogen deprivation during the timelapse experiment, ensuring the continuation of the meiotic program (prophase and meiotic divisions).

Fluorescence microscopy timelapse

⏱ Timing: 5–6 h

⏱ Timing: 30 min -1 h (for steps 22 to 29)

⏱ Timing: 5 h (for step 30)

To observe specific structures like chromosomes and microtubules throughout the meiotic process, particularly using endogenous fluorescent protein tags, we employ fluorescence microscopy.

Note: To facilitate optimal image acquisition, set the required temperature in the microscope (28°C for efficient meiotic progression) at least 3 h before starting the timelapse. This gives the microscope sufficient time to reach the required temperature and allows it to maintain this temperature throughout the timelapse.

21. Prepare the necessary hardware for your microscopy system.

Note: We have used various microscopy systems for our research, including the Confocal Spinning Disk Dragonfly system by Andor-Oxford Instruments, the Confocal Spinning Disk system by Nikon, and the DeltaVision system by Applied Precision.

22. Initiate your microscopy software program.

Note: The image acquisition software used varies depending on the microscopy system. For example, the Confocal Spinning Disk Dragonfly system by Andor-Oxford Instruments uses Fusion, the Confocal Spinning Disk system by Nikon uses Metamorph by Molecular Devices LLC, and the DeltaVision system by Applied Precision uses SoftWorx.

23. Select the 100× objective (with immersion oil capability) on your microscope and apply a drop of immersion oil onto the objective.

Note: Coming into contact with immersion oil may lead to skin irritation.

24. Insert the microscopy chamber into the microscope stage with the appropriate adapter, ensuring that the medium is accessible (for adding drugs if necessary).

⚠ CRITICAL: this product (micro-slide 8 well slide, Ibidi) is only compatile with certain immersion oils (see compatible oils in product instructions or on www.ibidi.com). Otherwise, the slides could crack.

25. Move the objective towards the bottom of the chamber until you reach the focal plane where the cells are immobilized.
26. Choose multiple positions throughout the spot of previously immobilized cells (steps 15-20), seeking for obtaining the maximum number of meiocytes per field, which will depend on the efficiency of meiotic induction for each given strain (e.g., 2–5 meiocytes per field in our hands).

Note: Choosing positions containing the maximum number of meiocytes is strongly advised, since it will increase the efficiency of data acquisition during the timelapse.

Note: Choosing positions that are as close as possible to each other, as long as they are not overlapping, will reduce the time spent travelling between positions. This will maximize the

Table 1. Acquisition settings in Spinning Disk confocal system (Olympus/Yokogawa)

Fluorescence protein	Excitation/Emission	Laser power	Exposure time	z-stack	Time interval	Objective
CFP	445/452-45	10%	200 ms	14 sections 0.4 μm apart	3 min	100×/1.4 NA Oil Plan Apo
GFP	491/525-45	10%	200 ms	14 sections 0.4 μm apart	3 min	100×/1.4 NA Oil Plan Apo
m-Cherry	561/605-64	60%	200 ms	14 sections 0.4 μm apart	3 min	100×/1.4 NA Oil Plan Apo

number of positions that can be imaged for a given acquisition rate and/or minimize the acquisition rate.

△ CRITICAL: You ought to familiarize yourself with the setup of your microscopy system and the risk of photobleaching or phototoxicity due to fluorescence cross-incidence radiation between close positions.

Note: For example, to optimize the path between selected positions, microscopy software such as Fusion provides built-in algorithms. If your software lacks this option, you can implement a script that uses external or custom algorithms such as the nearest-neighbour method.[12]

27. Confirm that all positions remain in focus using a brightfield view before initiating the timelapse. If not, re-focus the correspondent position.

Note: Re-focusing all the taken positions before initiating the timelapse is important because as the last position is acquired, the first few positions may have become slightly defocused.

28. Activate the required laser lines and ensure they are passing through the sample.
29. In cases where you need to use drugs at the time of the filmation, add the necessary volume of drug to the medium before starting the timelapse.

△ CRITICAL: Ensure that the drug is added on top of the medium surface to prevent the generation of flow currents that could detach cells from the chamber bottom. It is important to avoid hitting the chamber with the pipette, as it can cause the selected positions to drift apart. It is recommended that during the addition of the drug, you monitor a live brightfield view of a selected position to check for drifting.

Note: For example, we have used fast-acting drug-based systems at the time of filmation, when meiocytes are progressing through meiotic prophase, such that it is ensured that the effect of the drug is achieved before the formation of the spindle in meiosis I and II, to study the impact of these on spindle formation and/or function. For example, we have used the auxin-induced degron system to deplete specific proteins and latrunculin A to disrupt the F-actin network in this context, adding the drug just before starting the timelapse, with no incubation periods.[2]

30. Initiate the timelapse acquisition.

Note: For example, with the Confocal Spinning Disk Dragonfly system, we can record ten positions, using an acquisition rate of 5 min^{-1} and taking 14 Z planes with a spacing of 0.4 μm between them covering three fluorescence channels during a total recording time of 5 h. This allows us to avoid significant bleaching and phototoxicity while ensuring that meiotic progression of meiocytes is not compromised. The fluorophores we have used are all

Table 2. Acquisition settings in Dragonfly 200 confocal system (Olympus/Andor)

Fluorescence protein	Excitation/Emission	Laser power	Exposure time	z-stack	Time interval	Objective
GFP	488/521-38	30%	50 ms	14 sections 0.4 μm apart	3 min	100×/1.45 NA Oil Plan Apo
m-Cherry	561/594-43	10%	50 ms	14 sections 0.4 μm apart	3 min	100×/1.45 NA Oil Plan Apo

endogenous (protein fusions) and they comprise CFP, GFP and m-Cherry. Please, refer to the Tables 1, 2, and 3 for further explanation on the settings of the timelapse, which are strongly dependent on the microscopy system used.

Note: It is advisable to verify if the selected acquisition rate is sufficient to capture images of all positions and to provide enough time to refocus positions during acquisition rounds.

Note: As temperature changes can cause defocusing, it is advisable to refocus all selected positions after adding a drug, as it may be at a different temperature than the medium or the microscope. Furthermore, periodic refocusing of selected positions may be necessary due to fluctuations in the microscope temperature.

Note: For example, the Confocal Spinning Disk Dragonfly system is equipped with the Perfect Focus System (PFS) feature, which automatically refocuses positions before each acquisition event. The PFS measures the difference between the current and initial coordinates (reference) using infrared light. If you are using a different microscopy system that does not have this feature, you may need to manually refocus the positions in the spare time between acquisition rounds.

Fluorescence imaging quality control

⏲ Timing: 15 min (for steps 31 to 34)

Examine the acquired microscopy images to ensure they meet a set of criteria essential for subsequent analysis.

31. To obtain an initial overview of the timelapse, create a maximum projection of all *Z* planes for each position across all time points.

    Note: This can be achieved using the microscopy software or other image analysis software, such as ImageJ. Macros or plugins can be used to automate the process. The outcome will be a stack consisting of slices that display the maximum projection of each corresponding time point.

    Note: For example, the files obtained from timelapse acquisition with Fusion and Softworx software contain separate *Z* planes of all time points, while Metamorph generates separate

Table 3. Acquisition settings in Personal DeltaVision system

Fluorescence protein	Excitation/Emission	% Transmittance	Exposure time	z-stack	Time interval	Objective
CFP	436/470-30	32%	100 ms	14 sections 0.4 μm apart	3 min	100×/1.4 NA Oil Plan Apo
GFP	490/525-20	100%	250 ms	14 sections 0.4 μm apart	3 min	100×/1.4 NA Oil Plan Apo
m-Cherry	555/617-73	100%	500 ms	14 sections 0.4 μm apart	3 min	100×/1.4 NA Oil Plan Apo

files for each *Z* plane of each time point together with an .nd file that contains image metadata and an index of all generated files. Regardless of the acquisition software used, the maximum projections can be obtained using the open-source software ImageJ (also known as FIJI), along with the plugin "Metamorphnd& ROI files importer (nd stack builder)" (mm_nd_and_roi_pack.jar).

32. Carefully review the entire timelapse for any events that could affect the microscopy analysis, such as defocusing, drifting in the *XY* or *Z* planes, bleaching, phototoxicity, disturbances in meiotic progression, and other similar issues. These events can affect the quality and accuracy of the data, so it is crucial to address them before proceeding with any further analysis.
33. Verify that the range of acquired *Z* planes covers the entire vertical range of fluorescently labeled structures for each channel.

   Note: This can be achieved by ensuring that the uppermost and lowermost *Z* planes do not detect the fluorescence signal of the structure whereas the remaining planes do.

34. Ensure that the number and spacing of the acquired *Z* planes are appropriate to cover the entire fluorescent signal seamlessly. To do this, examine each individual plane and ensure that there is minimal overlap of the signal captured by that plane and its adjacent planes in the maximum projection.

   Note: This ensures that no signal is missed within the correct vertical range. This redundancy in signal capture also aids in identifying potential issues such as *XY/Z* drift or other artifacts when analyzing the maximum projection.

   Note: Performing checks is particularly crucial when imaging the spindle. As the spindle is a thin structure that can elongate significantly throughout the length of the cell, capturing the entire spindle body without gaps requires an adequate number and range of planes.

Self-assembled spindle analysis

⏱ Timing: 5 h (for steps 35 to 38)

Identify appropriate meiocytes and conduct an analysis of the structures of interest, primarily focusing on chromosomes and microtubules (the spindle).

35. Identify the meiotic cells (meiocytes) among the vegetative cells by looking for cells that are larger in size and have a bent shape (see Figure 2).
36. Evaluate the quality of the meiocytes, classifying each one in each position in the timelapse as suitable or unsuitable according to the following criteria:
   a. Meiocytes that are suitable (Figure 2) include:
      i. Meiocytes that result from complete fusion of mating cells and exhibit a bent shape with a thick middle part, which indicates the presence of a thick bridge joining the mating cells.
      ii. Meiocytes that have successfully completed karyogamy, resulting in the fusion of the nuclei of the mating cells into a single nucleus.
      iii. Meiocytes in the meiotic prophase stage, where the nucleus is surrounded by several fibers of astral microtubules that span the entire cytoplasm and oscillate between both tips of the meiocyte. In a wild-type case, the oscillating forces of microtubules are transmitted to the nucleus through the connection between telomeres and the SPB, resulting in horsetail movement where the nucleus follows this oscillatory movement. However, in the genetic background required for self-assembled spindle formation, the telomeres/centromeres are not connected to the SPB, causing the nucleus to not follow the
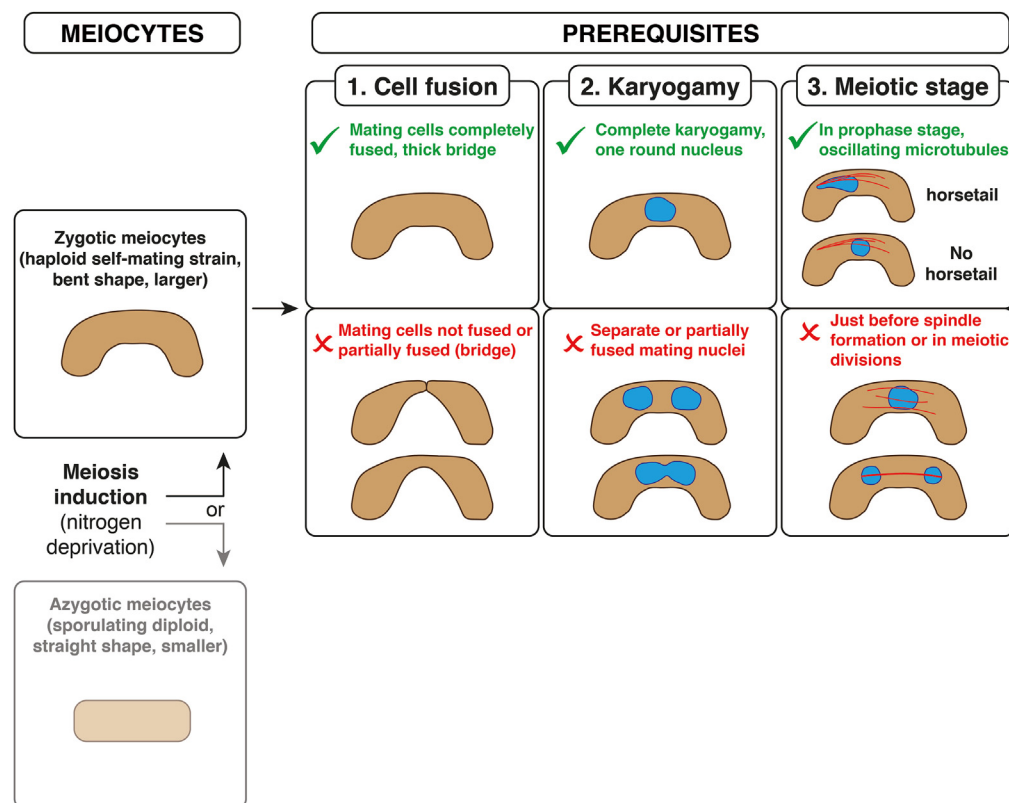
Figure 2. Prerequisites for selecting suitable meiocytes for analyzing spindle formation
The necessary conditions for fluorescence microscopy analysis of SPB-dependent and self-assembled spindles in fission yeast meiosis include obtaining and selecting meiocytes that are the required type and are in the appropriate stage of meiosis.

oscillatory movement (and thus no horsetail movement). Observing meiocytes in the meiotic prophase stage guarantees that the subsequent proper spindle formation has not yet occurred.

b. Meiocytes that are not suitable (see Figure 2) include:

i. Meiocytes that are formed early or immaturely, with unfused or partially fused mating cells that display an intact cell wall or a thin bridge between them. This can be observed through the brightfield channel.

ii. Meiocytes that may have correct cell fusion but have incomplete or partial fusion of the mating nuclei (karyogamy). This can be observed using fluorescent labeling of chromosomes, such as histone proteins.

iii. Meiocytes that are in a late meiotic phase, such as post-prophase, with several microtubule fibers surrounding the still nucleus at the center of the meiocyte or during the meiotic divisions (meiosis I or II), with the spindle already formed. In such cases, several structures may require labeling, including the nucleus (chromosomes or nuclear envelope) together with microtubules, depending on the observation method used.

iv. In our hands, we have not found any association between successful of meiosis progression or expected spindle behavior and the size of meiocytes. The final size of the meiocytes are the result of the size of the parental cells whose mating give rise to the meiocyte.

Note: To ensure that karyogamy is complete and stable and that nuclear movement is concordant with the background, it is recommended that the timelapse captures a minimum period of meiotic prophase (e.g., 30 min to 1 h). However, as the meiotic divisions span several hours,
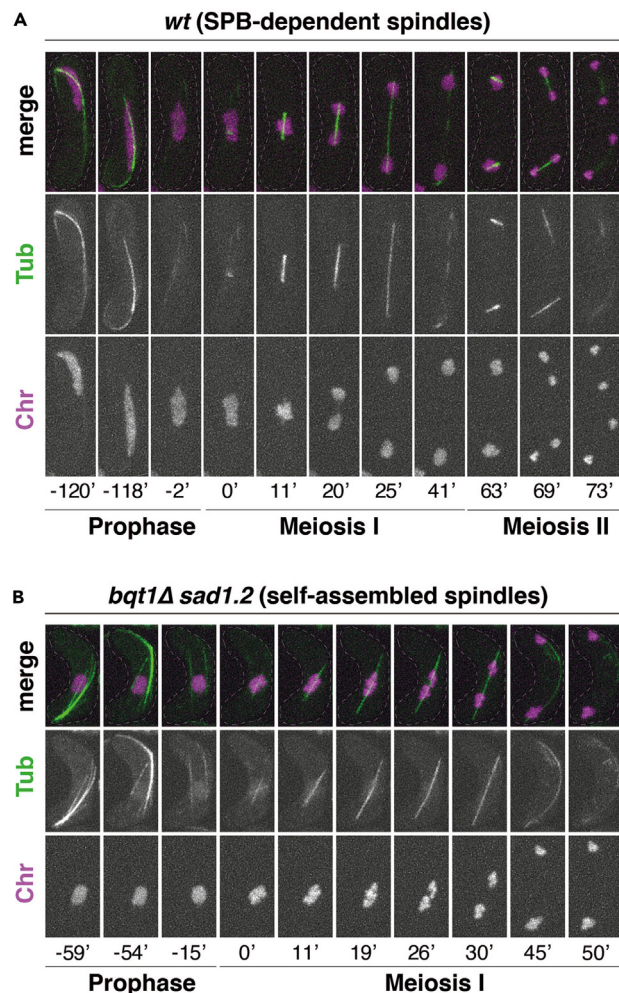
Figure 3. Examples of SPB-dependent spindles and self-assembled spindles in fission yeast meiosis

(A) Representative images of spindle and chromosome dynamics in a wild-type setting, where SPB-dependent spindles are formed.

(B) Representative images of spindle and chromosome dynamics in a *bqt1Δ sad1.2* mutant, where self-assembled spindles are formed. (A and B) Time stamps indicate the first frame in which spindle microtubules nucleate from a tubulin focus at the onset of meiosis I. The scale bars at the right of each panel represent 5 μm. The images are captured using fluorescent markers, where tubulin is labeled with leu1+::SV40-GFP-atb2 and chromosomes are labeled with hht1-RFP.

especially in the wild-type case, it is convenient to capture only the end of the meiotic prophase and not its entire duration.

37. Identify the window of time in which the spindle forms.

   Note: Observe the very end of the meiotic prophase, when the oscillating astral microtubules limit their movement and migrate from the tips to the center of the meiocyte, surrounding the static nucleus. As the microtubule fibers are dismantled, the nucleus will condense, and eventually microtubule filaments will begin to form within the nucleus, indicated by the tubulin signal in the vicinity of the chromosome signal. These filaments assemble into a rod-shaped bipolar structure, with a midbody and two poles, known as the spindle assembly. The spindle will then elongate, and the chromosomes will be segregated along the spindle axis in

opposite directions. Finally, the microtubules comprising the spindle will dismantle, resulting in the spindle disassembly, and the chromosomes will remain separated in several masses (see Figure 3).

38. Measure the length of the spindle body (see the quantification and statistical analysis section).

EXPECTED OUTCOMES

An ample concentration of meiocytes is needed to achieve successful meiotic induction. Ideally, this concentration would enable the observation of approximately 20–25 meiocytes within the field of view under a 40× objective when examining the sample on a slide before preparing it for fluorescence timelapse. When using the microscope camera, which typically has a narrower field of view than the 100× objective of the fluorescence microscope, a satisfactory concentration of meiocytes would yield a minimum of 2 meiocytes in the microscopy chamber.

To ensure sufficient statistical power for drawing meaningful conclusions, a successful timelapse should capture a minimum of 15 suitable meiocytes per session, based on the aforementioned criteria. These meiocytes should exhibit a brief initial phase of late meiotic prophase, complete meiotic divisions, and a short period thereafter to enable observation of spindle disassembly. By encompassing these stages, the timelapse can provide the comprehensive imaging necessary for quantitative analysis and for drawing reliable conclusions from a single session.

The obtained timelapse should have sufficient temporal and spatial resolutions to facilitate smooth observation of transitions between each meiotic stage and the key meiotic events. It should enable clear identification of various phenomena, such as the gradual slowdown and disappearance of oscillating microtubules, accompanied by chromosome condensation, indicating the transition from prophase to meiosis I. In addition, the formation of the spindle should be discernible as a distinct focus of the tubulin signal near the chromosomes, where microtubule filaments (one in the centrosomal type or multiple in the acentrosomal type) polymerize (spindle nucleation) and subsequently assemble into the complete spindle structure (spindle assembly). As spindle elongation progresses, the resolution should be sufficient to observe emerging discontinuities within the spindle body, followed by the dismantling and disappearance of the entire spindle structure.

When analyzing the spindle, monitoring the spindle length over time can provide valuable information regarding the quality of imaging. It is common to observe variability in the raw profiles of spindle length due to inherent differences in microtubule dynamics between individual spindles. To mitigate this variability, normalizing the spindle length to the size of the ascus (e.g., longitudinal ascus length) serves to standardize the profiles and establish a more defined, constrained trend. The trend of spindle elongation, represented by a line connecting the mean length at each time point, should exhibit a smooth, continuous increase throughout the duration of spindle observation.

It is important to note that abrupt changes in the shape of this trend line reflect the influence of individual data points that are more variable. In our experiments, we have observed such changes occurring around the later time points, where there are fewer data points representing the trend and thus greater variability. Recognizing this phenomenon is beneficial in identifying the meaningful segment of the trend line for the purpose of mathematical fitting.

QUANTIFICATION AND STATISTICAL ANALYSIS

Here we describe how to measure the spindle length and we provide the criteria to determine whether an observed spindle is SPB-dependent or self-assembled.

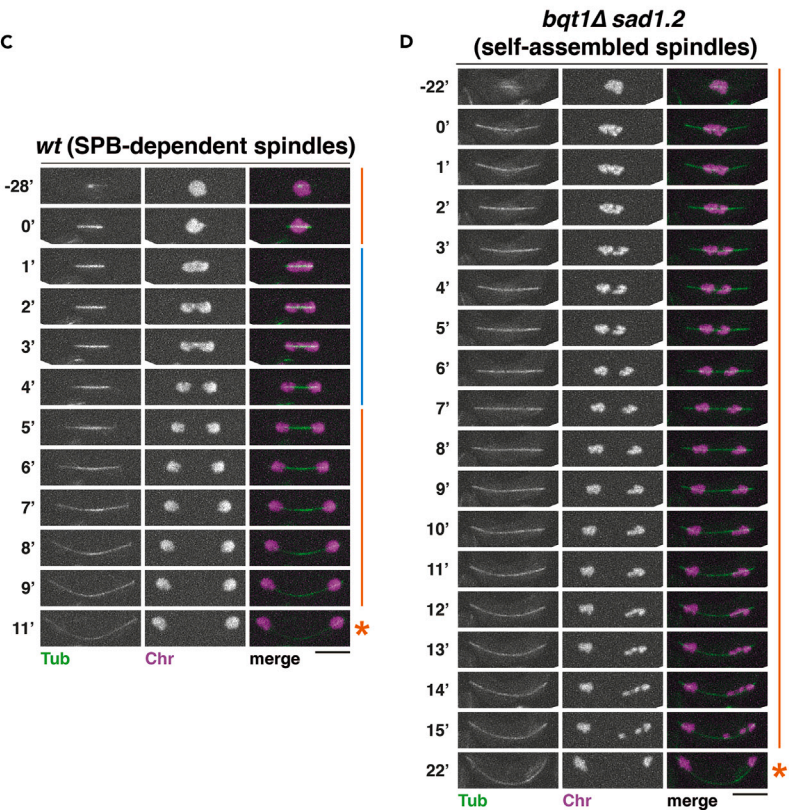**Spindle nucleation / assembly**
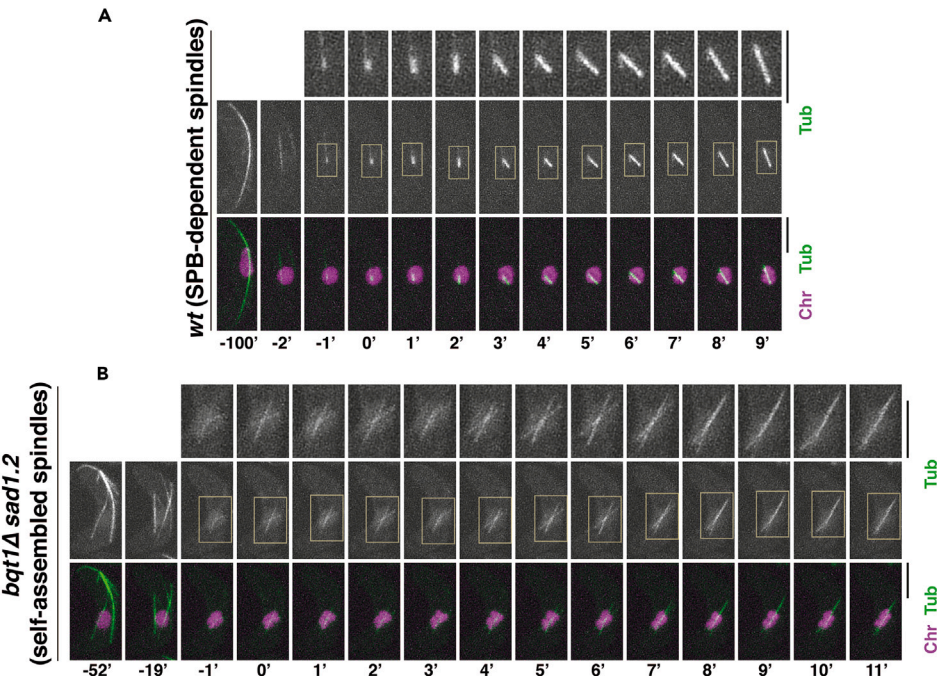
Chromosome segregation

Figure 4. The criteria for identifying and distinguishing between SPB-dependent and self-assembled spindles include differences in spindle nucleation and assembly, as well as chromosome segregation

(A and B) Time stamps from the first frame in which spindle microtubules nucleate from tubulin foci, with yellow rectangles showing the spindle body.

(C and D) Time stamps from the first frame in which chromosomes start segregating towards the spindle poles, with orange lines indicating periods of spindle elongation and blue lines depicting periods of chromosome movement towards the spindle poles. The orange asterisks mark the frame of maximum spindle length before disassembly. Tubulin (leu1$^+$::SV40-GFP-atb2) and chromosomes (hht1-RFP) are labeled. Proper selection and timing of meiocytes are necessary for fluorescence microscopy analysis of SPB-dependent and self-assembled spindles. The scale bars represent 5 μm.

Spindle length measurement

Spindle length can be measured manually with an image analysis software such as ImageJ/FIJI. With a decent-quality fluorescence images (signal-to-noise ratio ≥ 1.5 and pixel intensity dynamic range ≥ 12 bits), we define the spindle body length as the length along the microtubule array between their extremes. This measurement can provide information about potential defects in microtubule dynamics, checkpoint activity, nuclear envelope integrity, and other related factors. Several parameters can be derived from this measurement, such as the elongation velocity, the duration of the different stages of meiotic divisions, the maximum spindle length, and the time of spindle disassembly. Consider also examining the angle of spindle orientation, the position of spindle poles, the number and position of kinetochores, the chromosomal alignment, and the segregation accuracy of chromosomes. These analyses can provide insights into the function and regulation of the spindle in meiosis.

Criteria for spindle classification

We can differentiate the formation of the self-assembled spindle from that of the SPB-dependent spindle using three criteria:

1. Spindle assembly:

In the case of the SPB-dependent spindle, spindle microtubules initially emerge from a tubulin focus that is dot-like and located near the chromosomes. This tubulin focus quickly assembles into a well-defined, rod-shaped structure that continues to elongate (see Figure 4, shown in yellow rectangles).

In the case of the self-assembled spindle, spindle microtubules emerge from a diffuse tubulin focus as one or more pre-formed microtubule filaments with loosely defined midzone and poles. These filaments gradually collapse into a defined, rod-shaped spindle (see Figure 4, shown in yellow rectangles).

2. The alignment and separation of chromosomes relative to the elongation of the spindle:

Both SPB-dependent and self-assembled spindles are capable of segregating chromosomes, but the way in which chromosome segregation occurs in relation to spindle elongation varies between the two spindle types.

In the case of the SPB-dependent spindle, once it is assembled, it undergoes a subtle elongation (see Figure 4A, upper orange bar) before slowing down or stopping to maintain a relatively constant length of approximately 25% of its maximum length. During the elongation time, the chromosomes segregate towards opposite poles of the spindle in what is known as anaphase A (Figure 4, blue bar). The spindle then resumes elongation at a higher rate, segregating the chromosomes towards the opposite tips of the meiocyte in anaphase B (Figure 4, lower orange bar) until it reaches its maximum length. The next and final stage is spindle disassembly (Figure 4C, orange asterisk).

By contrast, the self-assembled spindle does not exhibit a pause or slowdown in elongation from the start of its assembly (Figure 4B, orange bar). Instead, chromosome segregation begins at a variable
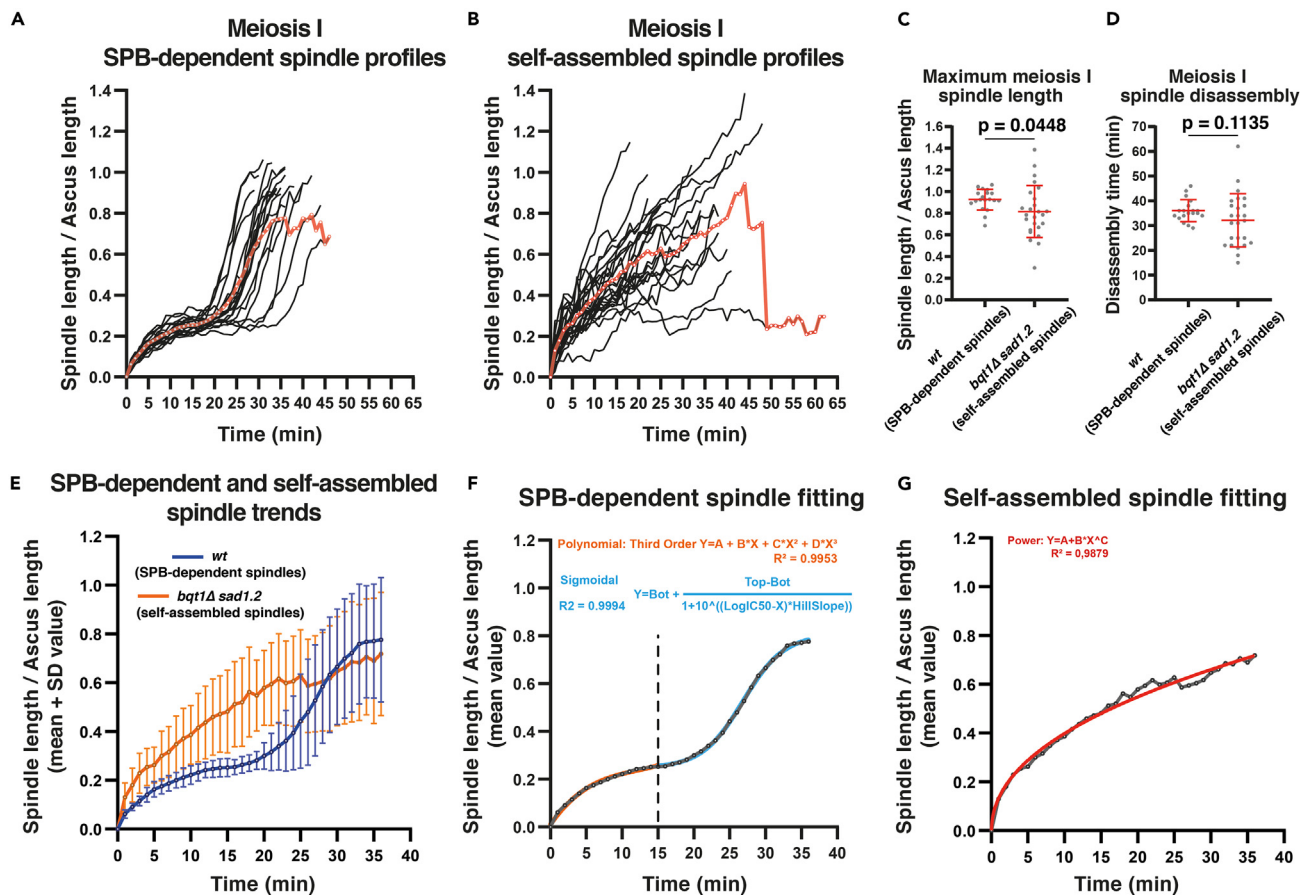
Figure 5. Analysis of differential elongation dynamics between SPB-dependent and self-assembled spindles

(A and B) Normalized length (spindle length over ascus length) profiles over time for SPB-dependent and self-assembled spindles, respectively. The black lines represent individual profiles, while the red line represents the mean of all individual profiles for each time point.

(C and D) Measurements of maximum meiosis I spindle length and spindle disassembly time, respectively. The p-value was determined using an unpaired t-test with Welch's correction for (C) and Mann Whitney test for (D).

(E) A comparison of normalized length profiles of SPB-dependent and self-assembled spindles, with mean (line) and standard deviation (bars).

(F and G) the non-linear fitting (color line) of mean normalized length (gray line) for SPB-dependent and self-assembled spindles, respectively. The polynomial third-order fitting was A = 0.01065, B = 0.04312, C = −0.003035, D = 8.397e-005. The sigmoidal fitting was Top = 0.8060, Bottom = 0.2466, LogIC50 = 26.84, HillSlope = 0.1511, IC50 = 6.891e+026, and Span = 0.5594. The power fitting was A = −0.009891, B = 0.1415, and C = 0.4587. Data was taken from 3 independent experiments.

point along the spindle axis during elongation (Figure 4D, blue bar), with chromosomes reaching the spindle poles towards the end of elongation, close to spindle disassembly (Figure 4D, orange asterisk).

3. Spindle dynamics:

By monitoring the length of the spindle over time, it is possible to consistently identify the three distinct stages of mitotic and meiotic SPB-dependent spindle dynamics: initial elongation, pause, and final elongation. By contrast, the self-assembled spindle appears to have only one persistent elongation stage, albeit with a variable rate. Although the time taken for both types of spindles to reach their maximum length is similar, the maximum length of the self-assembled spindle is slightly shorter than that of the canonical spindle (Figure 5).

Analyzing the overall trend of all individual elongation profiles can reveal distinct patterns of spindle dynamics, which can be accurately modeled using specific non-linear models. The SPB-dependent

spindle, for example, is best described by a third-order polynomial (R2 = 0.9953) during the initial elongation phase, followed by a sigmoid curve (R2 = 0.9994) during the pause phase, while the self-assembled spindle is best modeled by a power function (R2 = 0.9896) (Figure 5F).

We have used Graphpad Prism 8 for statistical analyses necessary for these studies.

LIMITATIONS

A limitation of fluorescence live-cell imaging may be the need for an incubation chamber coupled to the microscope to ensure focus stability during timelapse. Otherwise, the user may need to refocus frequently during image acquisition.

In addition, the incubation chamber for temperature control enables to set a stable and optimum temperature for fission yeast meiosis. The speed of several cellular processes such as spindle assembly and disassembly depends on temperature. Thus, maintaining the same temperature for all experiments allows the user to compare the spindle dynamics from different samples or days of acquisition.

The use of fluorescence illumination in imaging meiotic cells can lead to phototoxicity, which can negatively affect or even hinder the progression of meiosis. This issue is particularly significant when filming chromosomes, especially if they are labeled with a fluorophore requiring near-UV radiation (e.g., cyan fluorescent protein (CFP), 445 nm), which has high energy for excitation. Phototoxicity can manifest as disrupted chromosome movements during prophase or arrest at a specific meiotic stage. The problem can be exacerbated when employing multiple fluorescence channels, even if they use less energetic radiation. As a result, the design of a timelapse experiment may be constrained by various factors, including the number and distribution of structures within the cell, the dynamic nature of the process under investigation, the number of fluorescence channels, the three-dimensional (Z-axis) resolution, and the acquisition rate. These factors need to be carefully evaluated to mitigate the adverse effects of phototoxicity while capturing the desired information.

The formation of self-assembled spindles in fission yeast meiosis necessitates the elimination of contacts between centromeres/telomeres and the SPB (see Figure 1). This step is crucial to prevent the assembly of an SPB-dependent spindle and enable the establishment of a self-assembled spindle. Based on our observations, we have found that specific mutations affecting microtubule dynamics can suppress the self-assembled spindle formation. These mutations limit the extent of oscillatory movement exhibited by the SPB, confining it to the central region of the cell where the non-horsetail nucleus is located. We speculate that this proximity between the nucleus and the SPB may enhance the likelihood of interactions between centromeres/telomeres and the SPB, thus rescuing the formation of an SPB-dependent spindle at the expense of a self-assembled spindle. Consequently, certain genetic backgrounds can compromise the population of analyzable meiocytes, specifically those that give rise to self-assembled spindles.

TROUBLESHOOTING
Problem 1
High or low cell density in the field.

Potential solution

- If the imaging field is too crowded with cells or cells are layered, repeat steps 17-19, taking less biomass of cells to resuspend. If the cells are layered, reduce the time for settling cells onto the lectin-coated well in step 18.
- In cases of low cell density, try to increment the cellular biomass in step 17 and wash the Ibidi well gently to remove non-adhered cells. Do not pipette medium directly over the adhered cells; instead, drop the medium down from one side of the well.

Problem 2
High number of zygotes that do not progress in meiosis.

Potential solution

- Filming zygotic meiocytes that have not completed karyogamy may result in lack of progression during meiosis due to potential checkpoint activation by laser irradiation before nuclei fusion. Try to select zygotic meiocytes in step 36 (taking an image of the nuclei) that have completed karyogamy before timelapse acquisition.
- In addition, high phototoxicity may block meiosis progression after karyogamy completion. Try in step 36 to low laser potency, transmitted percentage and/or exposure times. This will be specific for each microscopy system, and so, it is advisable to start from the lowest value possible offered by the given setup and increase this until these undesired effects are observed.

Problem 3
Low fluorescent signal or loss of fluorescent signal during the timelapse.

Potential solution
Try different fluorophores to tag the proteins of interest and choose the most suitable one.

For example, we have found when tagging tubulin that green fluorescent protein (GFP) has a better fluorescence intensity and less photobleaching than mCherry.

RESOURCE AVAILABILITY

Lead contact
Further information and request for resources and reagents should be directed to and will be fulled by the lead contact, Alfonso Fernández-Álvarez (alfonso.fernandez.alvarez@csic.es).

Materials availability
This study did not generate new unique reagents.

Data and code availability
The published articles, Pineda-Santaella and Fernández-Álvarez[1] and Pineda-Santaella et al.[2] include all datasets analyzed during this study.

AUTHOR CONTRIBUTIONS
Conceptualization, A.F.-A., A.P.-S.; Methodology, A.F.-A., A.P.-S., R.M.-G.; Formal Analysis, A.P.-S.; Investigation, A.F.-A., A.P.-S.; Resources, A.F.-A.; Writing – Original Draft, A.F.-A., A.P.-S., R.M.-G.; Writing – Review & Editing, A.F.-A, A.P.-S., R.M.-G.; Supervision, A.F.-A.; Project Administration, A.F.-A.; Funding Acquisition, A.F.-A.

DECLARATION OF INTERESTS

The authors declare no competing interests.

REFERENCES

1. Pineda-Santaella, A., and Fernández-Álvarez, A. (2019). Spindle assembly without spindle pole body insertion into the nuclear envelope in fission yeast meiosis. Chromosoma *128*, 267–277. https://doi.org/10.1007/s00412-019-00710-y.

2. Pineda-Santaella, A., Fernández-Castillo, N., Jiménez-Martín, A., Macías-Cabeza, M.D.C., Sánchez-Gómez, Á., and Fernández-Álvarez, A. (2021). Loss of kinesin-8 improves the robustness of the self-assembled spindle in Schizosaccharomyces pombe. J. Cell Sci. *134*, jcs253799. https://doi.org/10.1242/jcs.253799.

3. Leupold, U. (1993). In The Origin of Schizosaccharomyces pombe Genetics, a.P.L.M. N. Hall, ed. (NY: Cold Spring Harbor Laboratory Press), pp. 125–128.

4. Fernández-Álvarez, A., and Cooper, J.P. (2017). Chromosomes Orchestrate Their Own Liberation: Nuclear Envelope Disassembly. Trends Cell Biol. *27*, 255–265. https://doi.org/10.1016/j.tcb.2016.11.005.

5. Tallada, V.A., Tanaka, K., Yanagida, M., and Hagan, I.M. (2009). The S. pombe mitotic regulator Cut12 promotes spindle pole body activation and integration into the nuclear envelope. J. Cell Biol. *185*, 875–888. https://doi.org/10.1083/jcb.200812108.

6. Tamm, T., Grallert, A., Grossman, E.P.S., Alvarez-Tabares, I., Stevens, F.E., and Hagan, I.M. (2011). Brr6 drives the Schizosaccharomyces pombe spindle pole body nuclear envelope insertion/extrusion cycle. J. Cell Biol. *195*, 467–484. https://doi.org/10.1083/jcb.201106076.

7. Fernández-Álvarez, A., Bez, C., O'Toole, E.T., Morphew, M., and Cooper, J.P. (2016). Mitotic Nuclear Envelope Breakdown and Spindle Nucleation Are Controlled by Interphase Contacts between Centromeres and the Nuclear Envelope. Dev. Cell *39*, 544–559. https://doi.org/10.1016/j.devcel.2016.10.021.

8. Chikashige, Y., Tsutsumi, C., Yamane, M., Okamasa, K., Haraguchi, T., and Hiraoka, Y. (2006). Meiotic Proteins Bqt1 and Bqt2 Tether Telomeres to Form the Bouquet Arrangement of Chromosomes. Cell *125*, 59–69. https://doi.org/10.1016/j.cell.2006.01.048.

9. Fennell, A., Fernández-Álvarez, A., Tomita, K., and Cooper, J.P. (2015). Telomeres and centromeres have interchangeable roles in promoting meiotic spindle formation. J. Cell Biol. *208*, 415–428. https://doi.org/10.1083/jcb.201409058.

10. Moreno, S., Klar, A., and Nurse, P. (1991). Molecular genetic analysis of fission yeast Schizosaccharomyces pombe. Methods Enzymol. *194*, 795–823. https://doi.org/10.1016/0076-6879(91)94059-l.

11. Forsburg, S.L., and Rhind, N. (2006). Basic methods for fission yeast. Yeast *23*, 173–183. https://doi.org/10.1002/yea.1347.

12. Fix, E., and Hodges, J.L. (1951). Discriminatory Analysis. Nonparametric Discrimination: Consistency Properties.